



Contents lists available at ScienceDirect

International Journal of Rock Mechanics and Mining Sciences

journal homepage: www.elsevier.com/locate/ijmms

Contribution of mine borehole data toward high-resolution stress mapping: An example from northern Bowen Basin, Australia

Mojtaba Rajabi^{a,*}, Moritz Ziegler^{b,c}, Oliver Heidbach^b, Saswata Mukherjee^a, Joan Esterle^a

^a School of the Environment, The University of Queensland, QLD, 4072, Australia

^b Technical University of Munich, 80333, Munich, Germany

^c Helmholtz Centre Potsdam, GFZ German Research Centre for Geosciences, 14473, Potsdam, Germany

ARTICLE INFO

Keywords:

Borehole breakouts
Borehole image log
Bowen basin
Drilling induced fractures
Stress map

ABSTRACT

Most of *in-situ* stress data in the Australian continent comes from wellbore stress analysis in deep hydrocarbon reservoirs, and earthquake focal mechanism solutions near the Australian plate boundaries, where geophysical tools facilitate understanding of the present-day stress patterns. This resulted in a paucity of stress information in many other regions such as the northern Bowen Basin, which is an active mining province, but with low seismicity rates and limited deep petroleum exploration. The mining industry runs several hundred kilometres of image logs annually to characterise geotechnical attributes. These logs provide an image from the borehole wall, which facilitates analysis of stress-related borehole deformations for *in-situ* stress characterisation. This paper examines the orientation of horizontal *in-situ* stress using different types of image logs in mine boreholes across the northern Bowen Basin. Analyses of 128 km of image logs in 680 vertical boreholes resulted in the interpretation of 9046 pairs of stress-related indicators including 735 drilling induced fractures and 8311 borehole breakouts. Our comprehensive database comprises 890 quality-ranked data records for the orientation of maximum horizontal stress (S_{Hmax}), which makes the Bowen Basin as a basin with the highest data density in the world in terms of quality-ranked stress information according to the World Stress Map. Statistical analysis of S_{Hmax} orientation reveals that the mean S_{Hmax} orientation in northern Bowen Basin is $N018^\circ \pm 16^\circ$. The results show that this orientation is consistent over long distances, which is in contrast with several eastern Australian basins. This uniform stress pattern agrees well with plate-scale geomechanical model predictions, which further highlights the impact of plate boundary forces in the contemporary stress pattern of this region. Detailed image log investigation did not show any systematic rotation of stress; however, some small-scale stress perturbations were observed in the vicinity of sharp stiffness contrasts and geological structures.

1. Introduction

The state of *in-situ* stress in the continental intraplate regions is generally thought to be consistent over vast distances, i.e., thousands of kilometres.^{1,2} However, several case studies from across the world have shown that intraplate stresses are not usually homogenous and can be perturbed by various stress sources at different spatial scales.^{3–6}

The Australian continent is a typical example of an intraplate region, exhibiting a significant variability in stress patterns across different spatial scales.^{5,7,8} In eastern Australia, for instance, the orientation of maximum horizontal stress (S_{Hmax}) differ, ranging from NNE-SSW in the northeastern part to ENE-WSW in the central-eastern region, and NW-SE in the southeastern area (Fig. 1). Apart from these regional stress

orientation variabilities, there are numerous smaller-scale stress re-orientations observed at basin, field, and borehole scales. For example, previous studies have shown stress perturbations due to the presence of small-scale geological structures in the southern Bowen and Surat basins,^{9–12} Clarence-Moreton Basin,¹³ Gunnedah and Sydney basins.^{14–16} Hence, a detailed stress analysis is essential to comprehend both the regional and local stress patterns in an area since the regional stress field may not necessarily reflect the present-day stress state at smaller scales. Likewise, stress analyses in only a few boreholes might not accurately represent the regional stress pattern.^{5,6}

In contrast to regions located near tectonic plate boundaries, where frequent earthquakes offer ample opportunities to analyse *in-situ* stresses, plate interiors experience limited and sparse seismic activity.¹⁷

* Corresponding author.

E-mail addresses: m.rajabi@uq.edu.au, m.rajabi@hotmail.com (M. Rajabi).

<https://doi.org/10.1016/j.ijmms.2023.105630>

Received 5 September 2023; Received in revised form 13 December 2023; Accepted 20 December 2023

Available online 28 December 2023

1365-1609/© 2023 The Authors. Published by Elsevier Ltd. This is an open access article under the CC BY-NC-ND license (<http://creativecommons.org/licenses/by-nc-nd/4.0/>).

Hence, stress analysis in such areas heavily relies on alternative methods, such as borehole stress analysis and engineering techniques (e. g., overcoring and hydraulic fracturing in civil and mining projects). Australia with 2150 stress data records is considered as one of the well-studied regions for *in-situ* stress analysis.⁵ However, 64 % of this data is from boreholes in mature petroleum basins, 30 % inferred from earthquake focal mechanisms, mainly near the boundary of Australian Plate, and only 6 % from mining and civil engineering sites.⁵

Mining is one of the main industries in Australia where there are over 300 operating mines in different parts of the continent,²⁰ and mining companies runs several hundred kilometres of image logs annually for their geological and geotechnical analysis.²¹ However, in the public domains, there is not much *in-situ* stress information in mining regions in Australia. For example, the northern Bowen Basin which is considered as the richest coal basin in Australia is represented by only 26 reliable S_{Hmax} data records in the latest release of the Australian Stress Map project.^{5,14,15,22} This sparse *in-situ* stress data in the public domain means that the stress pattern of this area is poorly understood. Even the available stress data shows different trends for the S_{Hmax} azimuth including N-S, NE-SW, NW-SE, and ENE-WSW orientations (Fig. 2). In addition, statistical analysis of stress data revealed that there is a 60° clockwise rotation of S_{Hmax} orientation from northern Bowen to southern Bowen and Surat basins (Fig. 1).^{6,23} Hence, understanding of the stress pattern in northern Bowen Basin is important for numerous implications including safety and stability assessment of mines such as slope stability, rock burst, designing the layout of mine workings,

excavation methods, and details of support.²⁴⁻²⁹ The *in-situ* stress also poses significant control on subsurface fluid flow, induced seismicity, fault reactivation, and fracture propagation in geo-storage sites and geo-reservoirs.^{5,30,31} Finally, such knowledge provides important information to understand how northern and northeastern boundaries of the Australian Plate control the stress pattern of northeastern Australia (Fig. 1).

This paper aims to improve the knowledge of the stress state in the northern Bowen Basin. Such knowledge has direct implications in safety and sustainability of mining operations in this region. Therefore, we systematically analyse borehole image logs in different mines of northern Bowen Basin. We analyse 680 image logs including 556 Acoustic Televiewers (ATV), 4 Optical Televiewers (OTV) and 120 resistivity-based image logs to examine the stress orientation pattern of this region. In particular, our study examines borehole breakouts (BOs) and drilling induced tensile fractures (DIFs) to determine horizontal stress orientations. We calculate the horizontal stress azimuth in each borehole and determine the mean regional S_{Hmax} orientation in the study area. We then use statistical methods and smoothing tools to calculate a reliable mean S_{Hmax} orientation and its standard deviation on a regular grid in the region.³² Finally, we conduct detailed statistical analyses on point-wise data to understand the horizontal stress variabilities in different depth intervals of the northern Bowen Basin. Given the closely spaced nature of boreholes in the mining industry, this study offers a unique opportunity to explore stress variability across a wide range of scales, from a very small-scale to the basin-wide level.

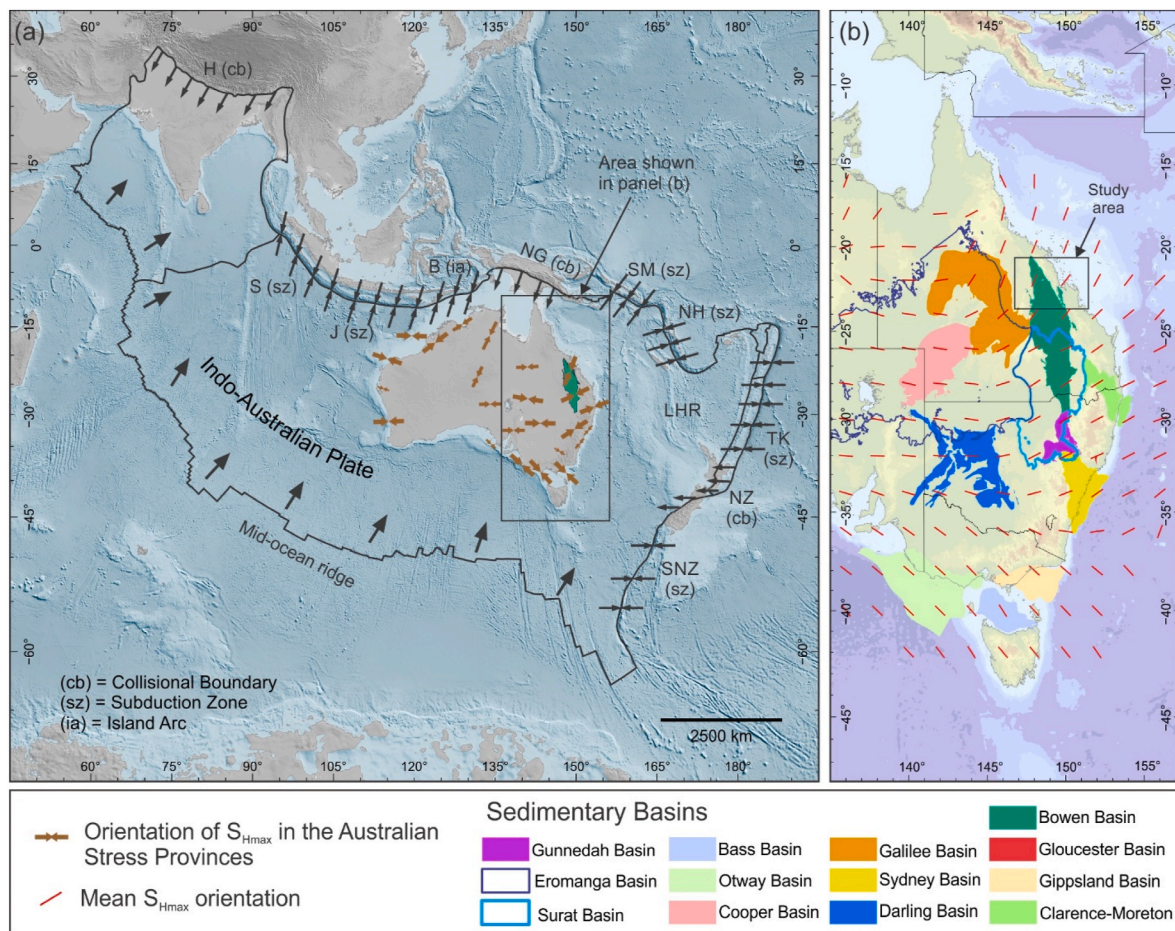


Fig. 1. (a) Location of the Bowen Basin in relation to the present-day tectonic setting of the Australian Plate, modified from .¹⁸ Note that force arrows are not drawn to scale. NZ, New Zealand; SNZ, south of New Zealand; TK, Tonga-Kermadec Trench; H, Himalaya; J, Java Trench; S, Sumatra Trench; NG, New Guinea; B, Banda Arc; NH, New Hebrides; SM, Solomon Trench; LHR, Lord Howe Rise. (b) Mean Orientation of maximum horizontal stress (S_{Hmax}) based on statistical analysis, in eastern Australian basins (modified from ⁵ and ⁶ Background images are from ¹⁹

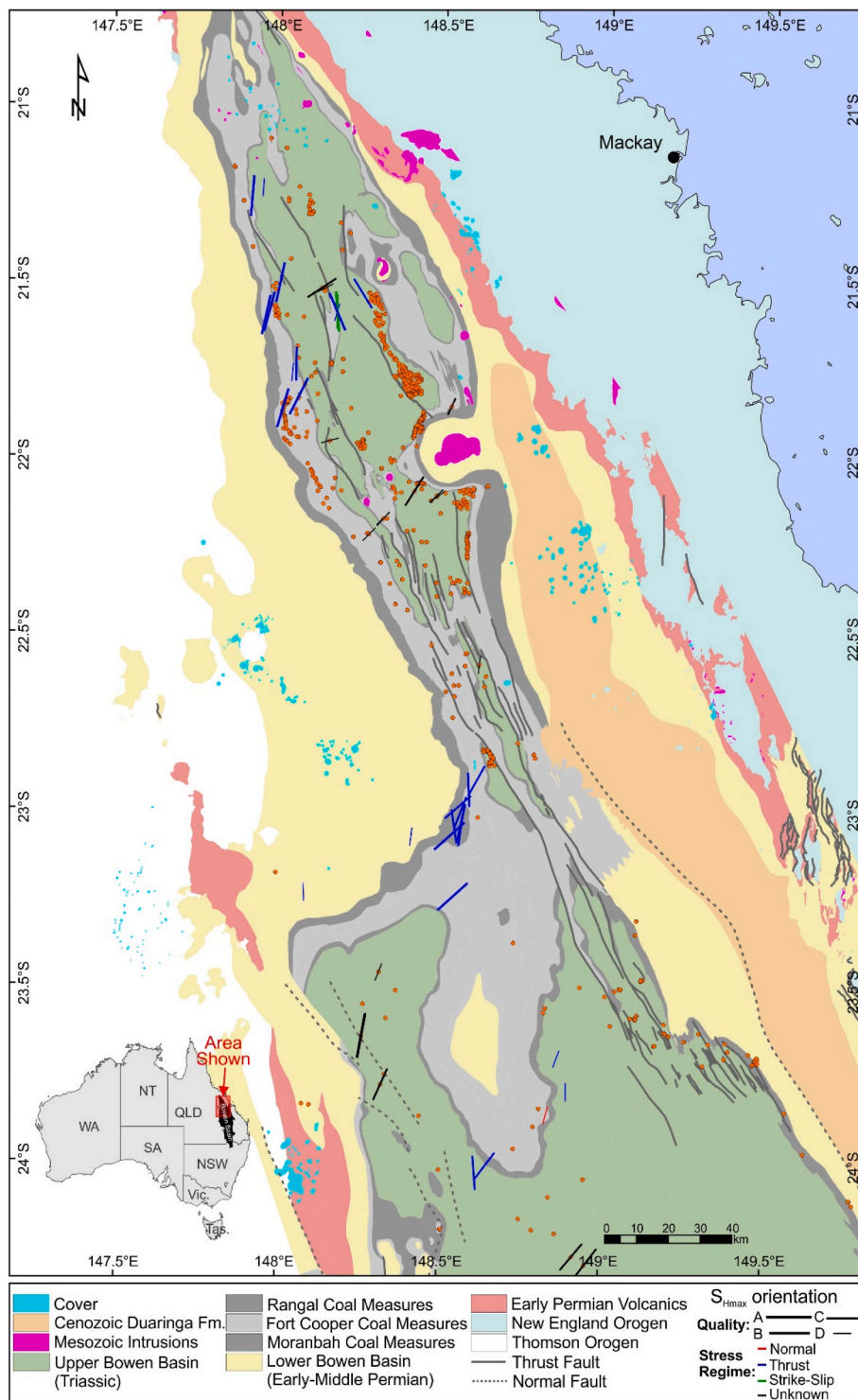


Fig. 2. Geology of northern Bowen Basin modified from ³⁴ and the state of *in-situ* stress orientation in the area prior to this study from ⁵. Colours for *in-situ* stress indicators represent stress regimes. Azimuth of each line shows the orientation of maximum horizontal stress (S_{Hmax}), and length of the lines shows the quality of the data (from A to D) based on the World Stress Map ranking scheme.⁴⁰ Limited stress information in this area shows variations of S_{Hmax} orientation. Orange dots shows the location of studied boreholes in this study (i.e., 680 boreholes). (For interpretation of the references to colour in this figure legend, the reader is referred to the Web version of this article.)

2. Geological setting of the Bowen basin

The Permo-Triassic Bowen Basin is a significant energy-rich basin in eastern Australia that covers a North-South distance of >1000 km with a maximum width of ~250 km. It contains a substantial sedimentary fill of up to 10 km.^{33–35} The basin is a part of the Sydney-Gunnedah-Bowen

basins system in eastern Australia that extends from northern Queensland to southern New South Wales (Fig. 1).³⁵ The basin is considered as one of the most important basins in Australia for its potential in energy, resources, and CO₂ storage.^{22,36–39}

From at least as far back as the Cambrian through to the Early Cretaceous, the eastern Australian continental margin was characterized

by subduction.⁴¹ The subduction process was complex, with episodes of accretion, slab retreat leading to widespread crustal extension and slab advance causing thick-skinned thrusting and crustal loading as reviewed and discussed by Donchak, Purdy, Withnall, Blake, Jell.⁴² The Bowen Basin developed in a continental back-arc setting during the Early Permian to Mid-Triassic in response to first crustal extension, then thermal relaxation and foreland loading.⁴³ Fig. 3 summarises the basin's structural history from its inception to the present-day.

During the early Permian, rift-controlled extension caused abundant volcanic activity to the east of the future Bowen Basin and formed numerous fault bounded grabens and half-grabens filled with thick fluvial and lacustrine sediments including rare thick coal seams.⁴⁴ Some of the rift basins occur at the base of the Bowen Basin, while others are entrained in the basement terranes to the east. Rifting subsided and was followed by a period of thermal relaxation that was associated with a regional marine transgression across the Bowen Basin.⁴⁵ The surviving

basin fill from this time includes sandy deltas in the west and marine shelf deposits in the west, suggesting that much of the eastern part of the basin has been eroded.

A prolonged period of intermittent compression, the Hunter-Bowen Orogeny, started during the late Permian with the stacking of thick thrust sheets in the eastern basement terranes, causing foreland loading in the Bowen Basin.⁴⁶ As subsidence in the basin accelerated, marine sediments were followed by the thick coal measures that host most of Australia's coking coal wealth. Influx of sediments from the east eventually buried the coal measures, and fluvial/lacustrine deposits dominated the Bowen Basin until the Mid-Triassic.⁴⁵ A phase of east-west compression caused the mid-Triassic closure of the Bowen Basin, when regional-scale folds exposed basement and large isolated thrust faults with characteristic fault-bend folding. Most of the early Permian rift faults inverted during this time.⁴⁷

The final deformation event of the Hunter-Bowen Orogeny was a focussed ENE-WSW compression that resulted in over 1 km of uplift along narrow, 300 km long, fold-thrust belt. This belt runs along the current eastern margin of the basin and has a major impact on the coal fields in the study area. Along strike, the fold-thrust belt contains between 2 and 8 significant thrust faults across a 20–30 km wide zone. Individual faults are between 30 and 140 km long and have up to 1000 m throw. Deformation increases to the east, where tight folding becomes dominant.³⁴

After the Hunter-Bowen Orogeny, the Mesozoic to Cenozoic history of eastern Australia was relatively quiet. Subduction stepped out to the east, allowing the intracratonic Surat Basin to develop above the Bowen Basin.⁴⁸ Widespread siliciclastic volcanism and uplift during the Cretaceous was associated with rifting and later the opening of the Tasman Sea.⁴⁸ Several small intrusions and numerous dykes within the northern Bowen Basin are correlated with this event. Later the Durling Basin developed as a half-graben associated with the opening of the Coral Sea⁴⁹ that is superimposed on the Bowen Basin, probably inverting one of the late Hunter-Bowen thrust faults. Cenozoic hot-spot related volcanism was associated with widespread basalt lava flows across the Bowen Basin, several sheet volcanoes, and abundant dykes.⁴⁹ Since the late Cenozoic, Australia's drift to the north led to a collision with Papua New Guinea, setting up the present-day stress field.

3. Materials and methods

In this study, a comprehensive analysis of various borehole image logs, such as Acoustic Televiewer (ATV), Optical Televiewer (OTV), Fullbore Formation MicroImager (FMI), Compact Micro Imager (CMI), and Slim-hole CMI (SCMI), was conducted to interpret BOs and DIFs. In addition, a thorough literature review was undertaken, and stress data from 29 other boreholes in the northern Bowen Basin were compiled.^{5,11,14,15,50} Hence, this paper presents the horizontal stress orientations from 709 boreholes (i.e., 680 our own analysis and 29 boreholes from the literature) for the northern Bowen Basin (Fig. 2). Table 1 summarize the database and the sources of data for stress analysis in this paper. A brief introduction on the tools and methods that have been used in this study is explained below.

Table 1

A summary on the number and sources of data used for the analysis of S_{Hmax} orientation in the northern Bowen Basin. Note that if both breakouts and drilling induced fractures were picked in a single borehole, we report two S_{Hmax} orientations in that borehole, as suggested by the World Stress Map project.

Data sources	No. of boreholes	No. of data records for the S_{Hmax} orientation
Mine boreholes	537	644
Coal Seam Gas wells	143	216
Published literature	29	30
Sum	709	890

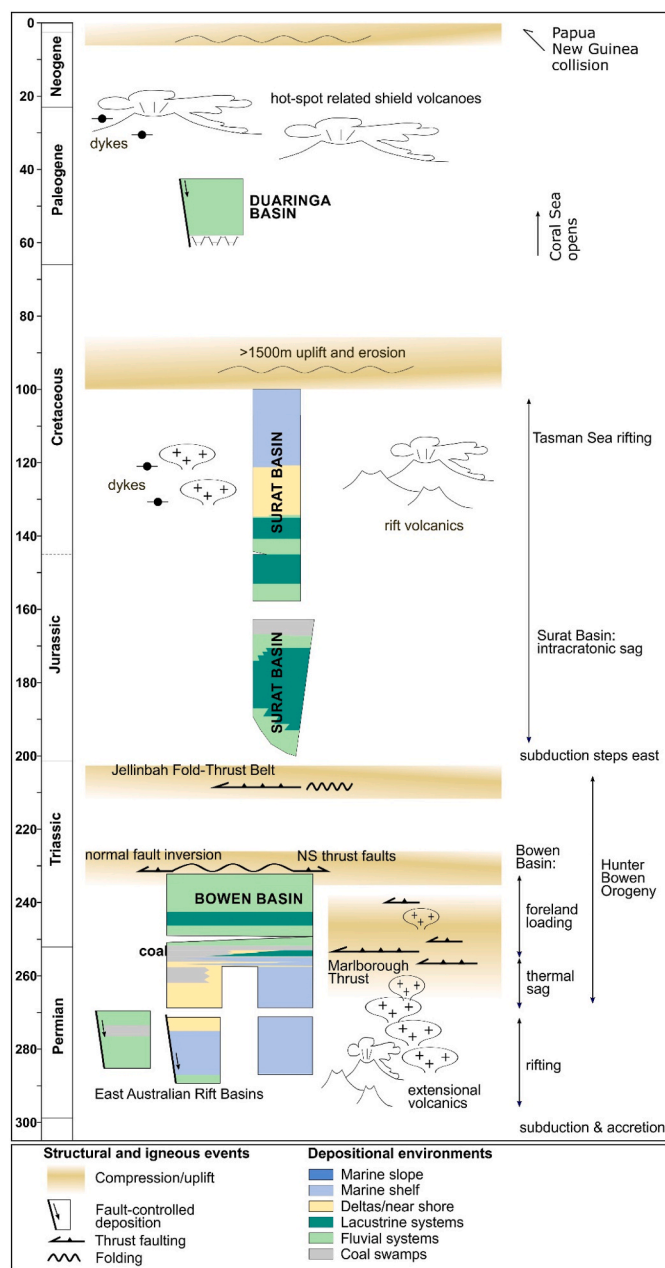


Fig. 3. Structural history of the Permo-Triassic Bowen Basin from its inception to the present-day.³⁴

3.1. Stress mapping approach

In geomechanics, the state of the stress is explained by the concept of the Cauchy stress tensor.^{51–53} Assuming that the overburden stress (i.e., vertical stress; S_v) is one of the three principal stresses, the minimum and maximum horizontal stresses (S_{hmin} and S_{Hmax} , respectively) are principal stresses as well. Hence, the 3D stress tensor is described with the magnitudes of S_v , S_{Hmax} , S_{hmin} and the orientation of S_{Hmax} .⁵²

Stress mapping is a visual representation for any of the stress tensor parameters that can visualise stress magnitudes,⁵⁴ stress orientations and stress regimes^{5,6}; and even pore pressure, which is an important parameter to understand effective stresses.⁵⁵ The use of stress maps has a long history and it has been used as a well-established approach to understand the stress pattern of a region and investigate the stress sources at different scales such as mine, field and basin,^{10–12,14,15,56,57} and even continental and global scales.^{6,8,40,58–60} Most of previous basin-scale stress orientation maps were primarily derived from petroleum borehole data, which were limited to specific intervals, such as reservoirs. In addition, conventional petroleum wells are usually having long borehole spacing that can cause significant uncertainty regarding the spatial and depth-related patterns of horizontal stress orientations. This study, however, employs mine borehole image log data, spanning from the near surface to a depth of 1.6 km. Notably, mine boreholes have close borehole spacing (sometimes <30 m), facilitating the creation of a high-resolution stress map both spatially and in terms of depth, ranging from the near surface to 1.6 km depth.

In this study, we map 890 S_{Hmax} orientation data records inferred from 709 boreholes to understand the stress pattern of this mining region. To be consistent with previous stress mapping projects, we calculate the mean S_{Hmax} azimuth for each borehole based on directional statistics.^{40,61} We then assign a quality (from A to E) to these S_{Hmax} orientations following the World Stress Map quality ranking scheme. A-quality is the most reliable data (the uncertainty of S_{Hmax} is believed to be within $\pm 15^\circ$), B (S_{Hmax} is believed to be within $\pm 20^\circ$), C (S_{Hmax} is believed to be within $\pm 25^\circ$), D (S_{Hmax} is believed to be within $\pm 40^\circ$), and E (S_{Hmax} in that borehole is not reliable as the standard deviation is $> \pm 40^\circ$ or the required information is incomplete). This quality ranking scheme enable us to compare S_{Hmax} orientations inferred from different methods.⁴⁰

3.2. Borehole image log analysis

Borehole images logs are 360° representation of borehole wall and are widely used in petroleum industry and more recently in mining sector for the analysis of subsurface structures.^{62–65} These logs come in various types, each tailored to different borehole environments.⁶⁵ Typically, these tools capture borehole images either directly, through optical methods like video or photography, or indirectly, based on physical properties of the surrounding rock and fluid, such as density, resistivity, and acoustics.⁶⁵ In this study, we utilized a range of image logs including acoustic-based (ATV), resistivity-based (FMI, CMI and SCMI) and optical-based (OTV) in 680 boreholes (Fig. 2). Image logs that sometimes are referred to as “optical cores” are considered as invaluable tool for characterisation of subsurface structures such as faults, fractures, and stress-related indicators in boreholes. Analysis of BOs and DIFs using image logs are considered as well-established methods for crustal stress analysis.^{56,62,66}

When a borehole is drilled, it removes a cylinder of rock that was originally providing support to the surrounding materials, which were under compression by far-field stresses. Consequently, the drilling operation leads to a re-distribution of stress on the borehole wall, potentially resulting in the formation of breakouts (BOs) and drilling induced fractures (DIFs) depending on the tensile and compressive strength of the drilled rock (Fig. 4).⁶⁶ DIFs appear on the borehole wall when the tangential stress is less than tensile strength of the rock. These features, which align with the S_{Hmax} orientation, can be interpreted as two vertical fractures on both side (\sim separated by 180°) of a vertical borehole, either as low amplitude fractures in ATV or conductive fractures in FMI/CMI logs (Fig. 4). However, it is crucial to note that in coal basins, there exists a significant risk of misinterpreting these features and cleats, which are natural vertical fractures in coal seams.^{57,63} In this study, we took precautions to avoid misinterpretations by cross-referencing the borehole image logs with core photos. This approach helped us ensure more accurate and reliable results, reducing the risk of misidentifications. Breakouts initiate when the circumferential (or hoop) stress exceeds the compressive strength of rock on the borehole wall.⁶⁶ This results in the circular cross-section of a vertical borehole transforming into an oval shape, with the long axis indicating the orientation of S_{hmin} (Fig. 4).⁶⁶ In borehole image logs, BOs are identified as poorly resolved (either low amplitudes zones in ATV or

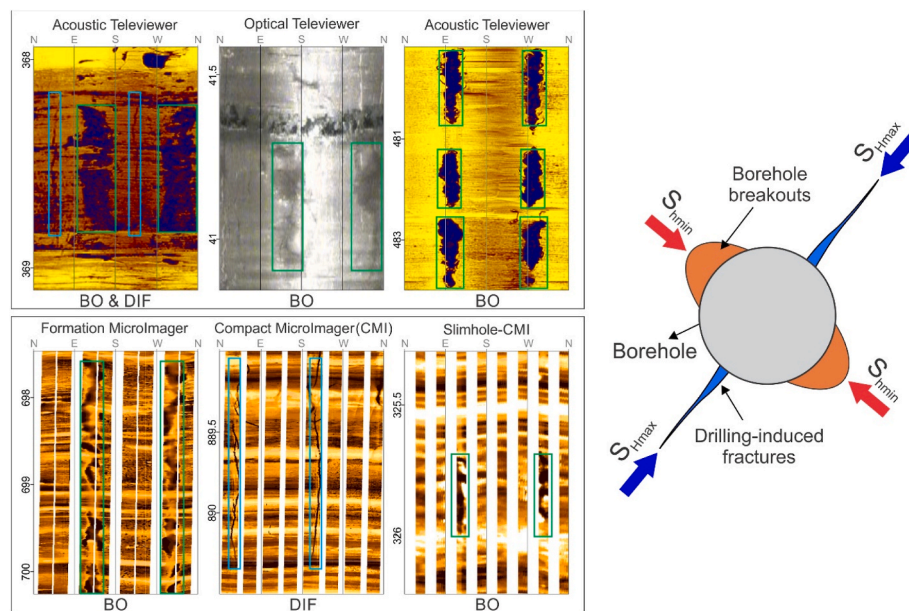


Fig. 4. Examples of drilling induced fractures (DIF) and borehole breakouts (BO) in different types of image logs in the studied boreholes. Schematic diagram (right) is a cross section of a borehole that illustrates the relationship between BO, DIF and minimum and maximum horizontal stresses (S_{hmin} and S_{Hmax} , respectively).

high conductive zones in FMI/CMI logs) forming on both sides of the borehole, separated approximately by 180° (Fig. 4). Not that all the boreholes studied in this study are vertical boreholes ($<10^\circ$ deviation), eliminating the need for additional corrections when determining horizontal stress orientations.⁶⁷ It should be noted that all the image log data have undergone through a strict quality control (QC) including borehole location and its magnetic declination, inclinometry QC to orient the image log (i.e., use True North as the reference of the image), applying different filters and corrections to improve the quality of image logs and make them interpretable for BOs and DIFs analysis. Although various methods such as automatic picking of features for image logs have been introduced, we interpreted and analysed all the image logs manually because some studies have shown that automatic picking occasionally fail to recognize certain features and often misinterpret and misclassify them.⁶⁸ More recently, Roshan et al.,⁶⁹ has introduced a new methodology to determine *in-situ* stresses using ATV logs without the requirements of borehole breakout analysis. However, in this study we analysed BOs and DIFs to be able to rank the mean S_{Hmax} orientation according to the World Stress Map guidelines.

3.3. Statistical analysis: stress province and search-radii stress analysis

In order to comprehend the basin-wide stress pattern of the study area, we employ two statistical methodologies: the stress province and search-radii technique. These approaches rely on directional statistics to calculate both the mean orientation of S_{Hmax} and its standard deviation, as explained below.

3.3.1. Stress province

The stress province is a method utilized in various releases of the Australian Stress Map project to assess the mean orientation of S_{Hmax} , standard deviation, and significance of stress orientations within a specific region.^{5,8} To apply this method, at least four S_{Hmax} data records should be available within close geographical proximity. High-quality data (i.e., data with higher quality according to the World Stress Map quality ranking), are given more weight in the statistical analysis.⁸ The next step involves calculating the mean orientation of the S_{Hmax} and the resultant vector length (*R-value*) for the Rayleigh Test, which assesses the randomness of the S_{Hmax} azimuth.^{61,70} In this process, a null hypothesis is defined, assuming that the S_{Hmax} azimuth in the region is random. Based on the null hypothesis and the R-value, six types of stress provinces can be classified: type 6 when the null hypothesis cannot be rejected at the 90 % confidence level, type 5 when it can be rejected at the 90 %, type 4 at the 95 %, type 3 at the 97.5 %, type 2 at the 99 %, and type 1 at the 99.9 %. Further details about this method can be found in Hillis and Reynolds;⁸ and Rajabi et al.¹³

3.3.2. Search-radii stress analysis: mean S_{Hmax} orientation on a regular grid

As mentioned earlier, stress maps offer pointwise and sparse information about the stress tensor's parameters. However, this approach lacks the ability to provide stress information beyond the measurement domain, resulting in stress data gaps. To address this limitation, various methods have been employed, including statistical analysis,^{32,40,70-72} and geomechanical stress modelling to predict the stress pattern in regions where there is limited (or no) stress data.^{7,73}

In this study, we employ the search-radii approach, a statistical method that is used to determine reliable mean S_{Hmax} orientations within a given standard deviation on regular grids.³² This method involves calculating the mean S_{Hmax} , considering the quality of the S_{Hmax} data records, as well as the distance to the grid point as weights.³² To implement this method, our criteria are that we expect a minimum of three S_{Hmax} data records with A-C quality are available in the variable search radii. The method starts with a search radius of 1000 km, decreasing by 100 km in each step. Then we plot the mean S_{Hmax} orientation on each grid point when the standard deviation is below 25° in the associated search radius. The search radius component of this

method is termed as the wavelength of the S_{Hmax} orientation, which is shown as background of the map.^{6,32} Hence, the final map shows the mean S_{Hmax} orientation with standard deviations $<25^\circ$ on regular grids along with the wavelength.

4. Results

We developed the stress orientation map of the northern Bowen Basin by analysing 128 km of image logs in 680 vertical boreholes (Fig. 5 and Table 1). In addition, we conducted a comprehensive literature review, gathering 30 S_{Hmax} data records from 29 other boreholes. This compilation included 20 data records from hydraulic fracturing measurements, 7 from overcoring tests,^{8,14,15,50} and 3 from image log analysis.¹¹ Hence, our stress analysis and data compilation yielded a total of 890 quality-ranked S_{Hmax} data records (Fig. 5, Table 2 and supplementary data). As a result, the Bowen Basin stress map stands as the most comprehensive, quality-ranked, basin-scale stress orientation map based on the World Stress Map database.⁶ Throughout our analysis, we interpreted a total of 9046 stress-related indicators, which included 8311 BOs and 735 DIFs across a depth range of 8 m–1600 m in the strata of the northern Bowen Basin.

Since individual S_{Hmax} indicators, inferred from BO and/or DIF, occur in different depth intervals of a borehole, a mean orientation of S_{Hmax} needs to be calculated from these indicators to represent the of S_{Hmax} orientation in that borehole. Generally, there are two methods (i.e., number-weighted and length-weighted) for the calculation of the S_{Hmax} orientation in boreholes.⁷⁴ For our analysis, we opted for the length-weighted approach, which assigns greater weight to the longer features (BOs or DIFs) when calculating the overall S_{Hmax} in each borehole. We then used the World Stress Map quality ranking scheme to rank all the S_{Hmax} orientations from A to E quality. Note that if both BOs and DIFs were picked in a single borehole, we reported two S_{Hmax} orientations in that particular borehole, as suggested by the World Stress Map quality ranking.⁴⁰

4.1. Statistical analyses of stress data: stress provinces

In the statistical analysis of stress province, we accorded greater weight to A-quality data, which is regarded as the most reliable S_{Hmax} data records. Conversely, we excluded E-quality data due to their lack of reliability.⁴⁰ Consequently, we assigned weights of 4, 3, 2, and 1 to A, B, C, and D-quality data, respectively. After conducting the statistical analysis using 659 A-D quality data points, we determined that the mean S_{Hmax} orientation for the northern Bowen Basin is $N020^\circ E$, with a standard deviation of $\pm 19^\circ$. With an R-value of 0.81, the null hypothesis can be rejected at the 99.9 % confidence level, signifying that the northern Bowen Basin is classified as a Type-1 stress province, based on the Australian Stress Map classification.^{8,13}

The stress map of the northern Bowen Basin represents a unique and comprehensive database of stress orientations. It includes stress data records derived from various stress indicators, such as borehole breakouts, drilling induced fractures, overcoring, and hydraulic fracturing measurements, each with different qualities. To investigate potential discrepancies between different datasets, we calculated the basin-wide mean S_{Hmax} orientations based on different datasets (i.e., different qualities and different stress indicators). In Fig. 6, we summarize the results of the statistical analysis for the different datasets. Notably, the mean S_{Hmax} orientations obtained from almost all the datasets exhibit a remarkable similarity, indicating a high level of agreement and consistency. This finding further highlights the reliability of the different stress indicators and qualities used to determine the basin-wide mean S_{Hmax} orientations.

4.2. Statistical analyses of stress data: search-radii methods

To predict a reliable mean S_{Hmax} orientation on a regular grid, we

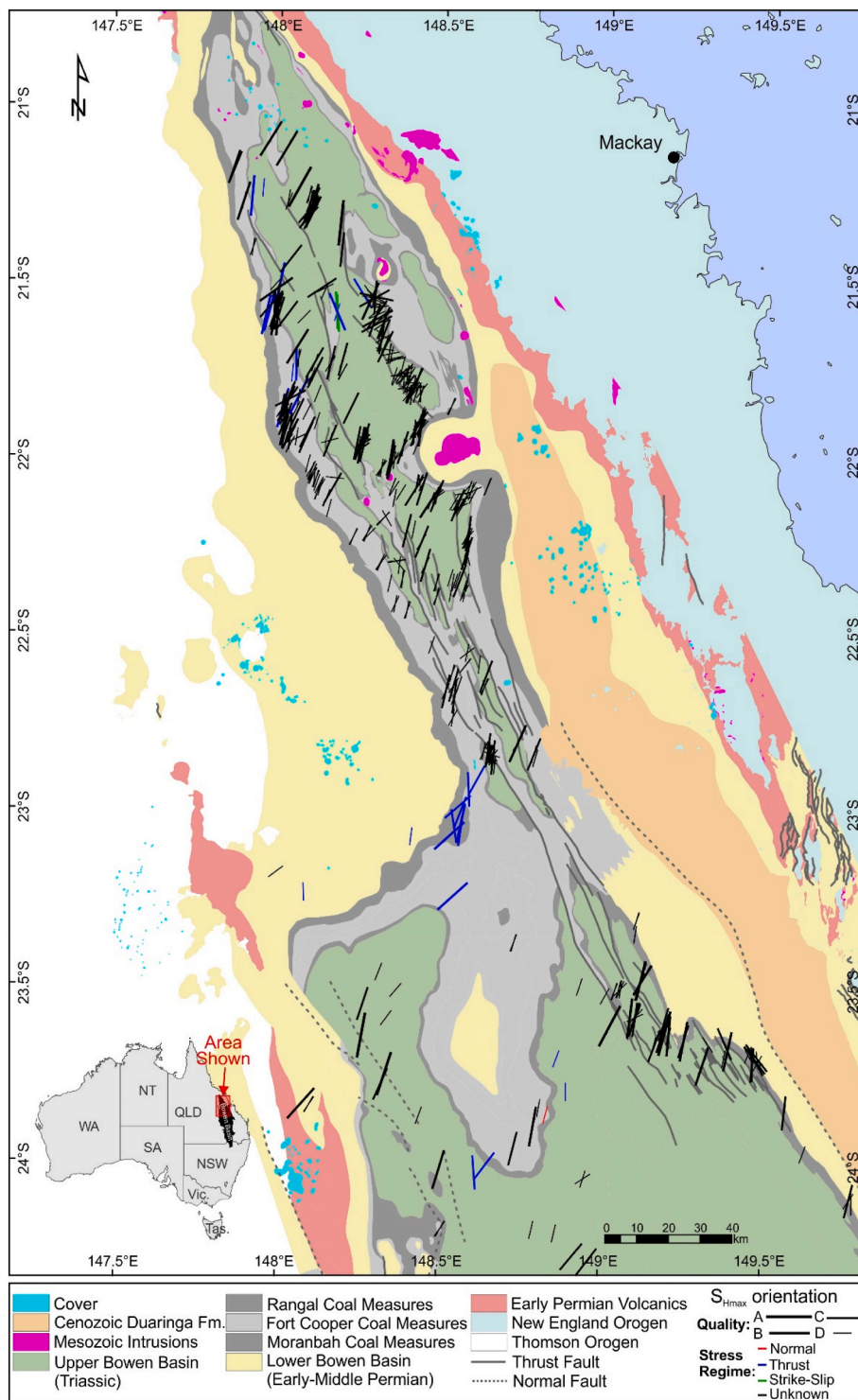


Fig. 5. Stress map of northern Bowen Basin using 890 quality-ranked orientation of maximum horizontal stresses. Azimuth of lines represent the orientation of S_{Hmax} , and length of the lines shows their quality (see legend). The background map shows the regional geology and geological structures of the area based on.³⁴

employed the search-radii method (see section 3.3.2). We conducted this analysis separately for both A-C and A-D quality data to see if the inclusion of D-quality data significantly impacted the results or not. The outcomes of the search-radii analysis are displayed in Fig. 7, which highlights a consistent mean S_{Hmax} orientation in the northern Bowen Basin for both A-C and A-D quality data. The wavelength analysis (background colour in Fig. 7a and c) appeared to be very long, exceeding 600 km in northern region, which then gradually decreased to shorter wavelengths (approximately ≤ 100 km) in the southern region. This

wavelength pattern provides valuable insights into the spatial consistency of the calculated mean S_{Hmax} orientation from each grid point. Shorter wavelengths indicate higher stress variability and local perturbations, suggesting regions with more localized stress variations. Conversely, longer wavelengths represent a more consistent pattern of stress orientations over long distances, implying greater regional stress homogeneity.

Table 2
Type and quality of the maximum horizontal stress orientations in northern Bowen Basin stress map. Quality is based on the World Stress Map ranking scheme.⁴⁰

Data Type	Number of quality ranked data					Total
	A-quality	B-quality	C-quality	D-quality	E-quality	
Borehole Breakout	7	23	100	314	231	675
Drilling induced fractures	0	0	4	184	0	188
Hydraulic fracture	0	10	9	1	0	20
Overcoring	0	0	0	7	0	7
Total	7	33	113	506	231	890

4.3. Stress orientations with depth

Large stress mapping projects have highlighted that, on average, there is no systematic or significant stress rotations with depths at large scales, such as tectonic plates and continental scales.^{5,6,75} These studies also show that there is no variation of the derived stress orientations derived from different methods. However, at smaller scales, various depth-wise systematic stress variabilities have been observed, primarily associated with the presence of mechanical detachment zones.⁷⁶⁻⁷⁸

In most basin-wide stress mapping projects, the focus is primarily on examining the spatial pattern of stress orientation and comparing S_{Hmax} orientations between individual boreholes. However, little attention has been given to the detailed analysis of stress orientation pattern from near surface to deeper intervals. A significant challenge in conducting a detailed depth analysis of stress data in basins is the lack of sufficient coverage of stress information from near-surface to deeper intervals.

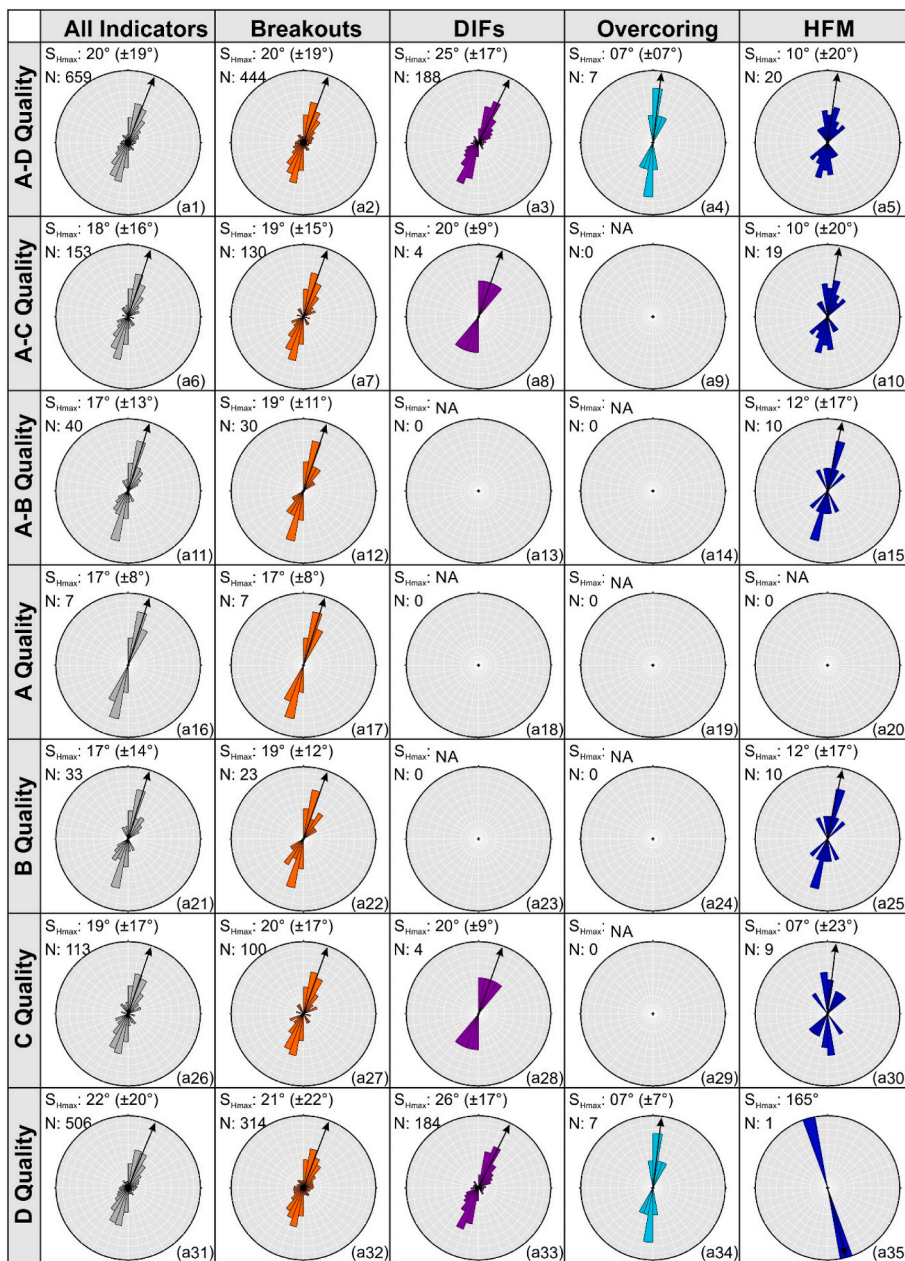


Fig. 6. Statistical analysis of maximum horizontal stress (S_{Hmax}) orientations using various datasets with different quality and data types. The calculated mean S_{Hmax} orientations for most data sets exhibit a high level of consistency, demonstrating agreement among the results. The only exception is the D-quality hydraulic fracture test, which consists of a single measurement and shows some deviation from the other datasets.

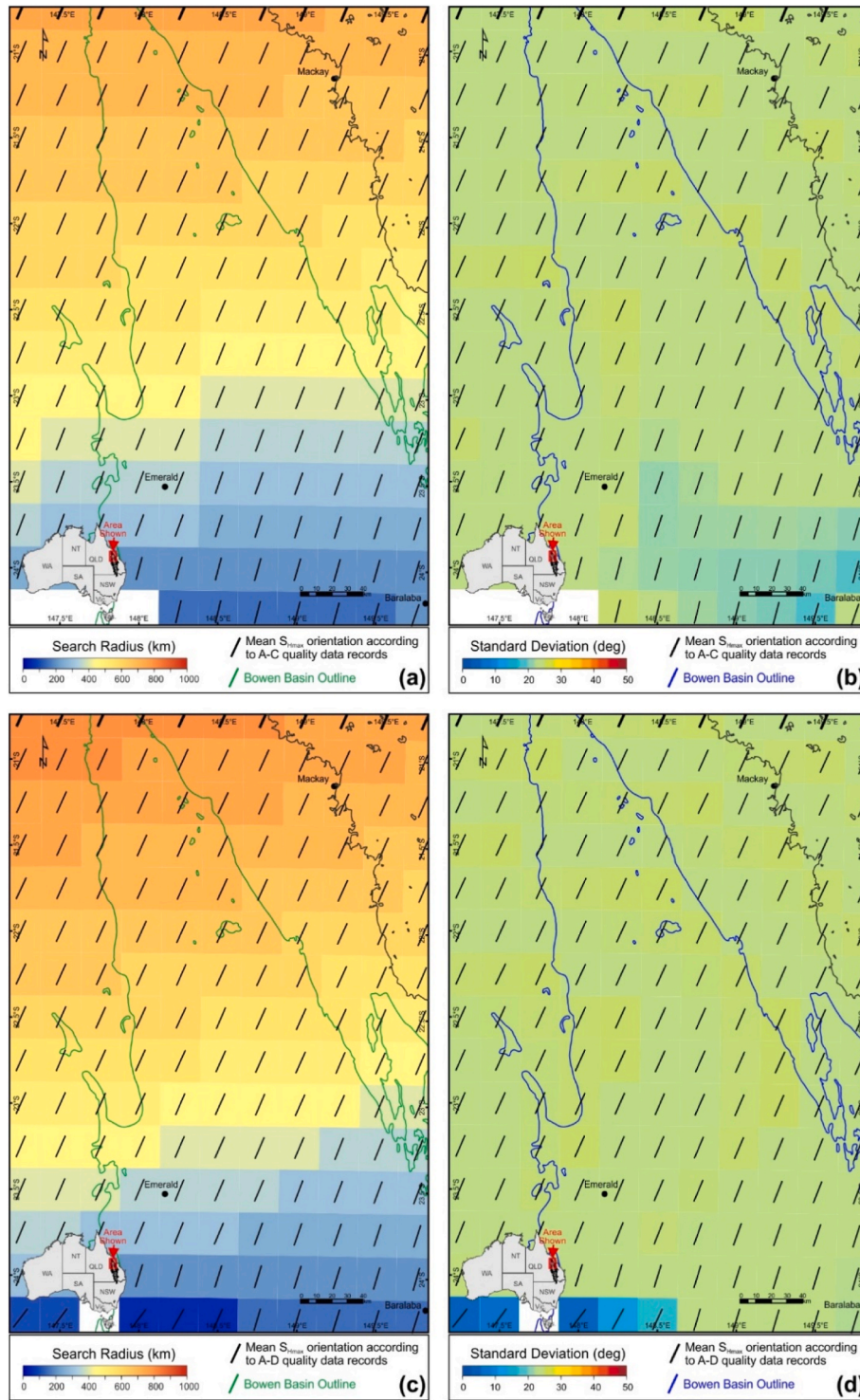


Fig. 7. Search-radii and wavelength analysis of the mean maximum horizontal stress (S_{Hmax}) orientation in northern Bowen Basin on regular grids using A-C quality data records (a and b) and A-D quality data records (c and d). The mean S_{Hmax} orientation is depicted by black lines. The background colour in (a) and (c) corresponds to the search radii that fulfil the search criteria used in this study ($\geq 3 S_{Hmax}$ data records, $< 25^\circ$ standard deviation for the mean S_{Hmax} orientation). The background in (b) and (d) illustrate the standard deviation of the mean S_{Hmax} orientation on grid points. In the northern part of the study area, the search radii exhibit a long wavelength (see a and c), indicating that the mean S_{Hmax} orientation remains consistent over significant distances. As we move towards the southern part of the area, the search radii transition into shorter wavelengths, as represented by blue colours (see b and d), meaning that the mean S_{Hmax} orientation in the southern part is consistent over shorter distances. (For interpretation of the references to colour in this figure legend, the reader is referred to the Web version of this article.)

This limitation arises because most image logs are typically run in specific intervals, such as reservoirs, and, hence, there is not enough coverage of stress information from near surface to do an extensive analysis.

In this study, the utilization of mine borehole data presented a unique opportunity to investigate the depth-wise pattern of stress orientation, spanning from near surface (approximately 8 m) to a depth of 1.6 km (Fig. 8). For the depth analysis of S_{Hmax} orientation, we plotted

all pointwise data, which included 9046 of S_{Hmax} orientation inferred from BOs and DIFs, 118 data records from HF and 7 data records from OC analysis. By calculating the mean S_{Hmax} orientation and standard deviation in 100 m intervals, we examined the stress orientation patterns throughout the depth range (near surface to 1.6 km) in the study area. Fig. 8 reveals a remarkable and consistent mean S_{Hmax} orientation in each interval and overall, despite the complex structural geology and tectonics of the basin, as well as the presence of coals with distinct mechanical properties relative to other strata in the basin. Note that in our study, most of the borehole are shallow boreholes (i.e., <700 m depth), and that resulted in more data in the shallower intervals (see last track in Fig. 8), meaning that the deeper intervals have been only covered by limited number of boreholes. For example, only 20 borehole

data were available for deeper than 1 km, while there were hundreds of boreholes for shallower than 700 m (Fig. 8). Hence, the stress orientations look more scattered in the shallower intervals, which we believe it is due to the data density and the inherent uncertainty in stress data analysis. Note that the statistical analysis of mean S_{Hmax} orientations shows small variations above and below 700 m (approximately 15° to 25°), which is within the standard deviation. Hence, our analysis indicates the absence of any systematic basin-wide variability of stress orientation with respect to depth in the northern Bowen Basin (Fig. 8).

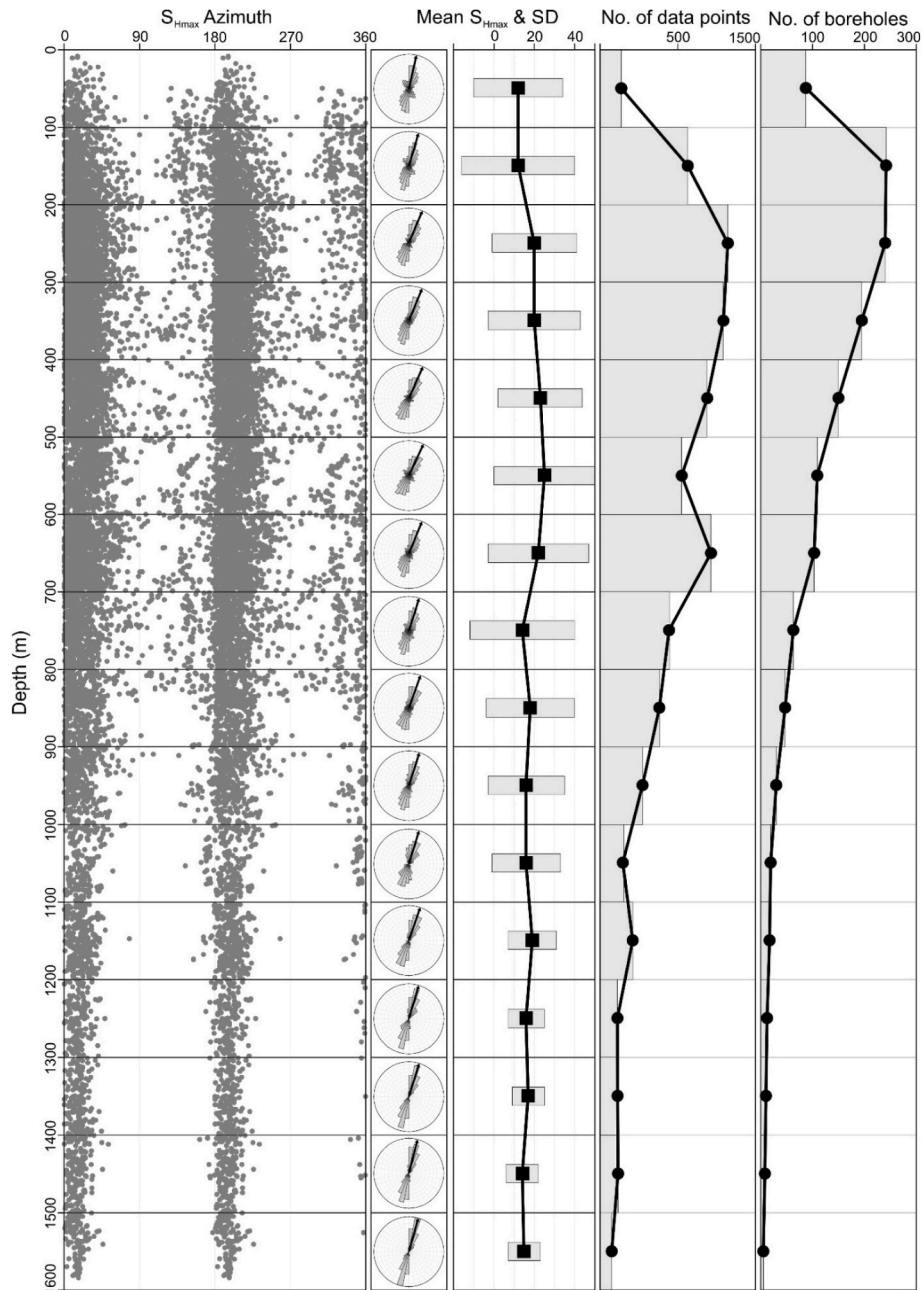


Fig. 8. The depth analysis of stress data in the northern Bowen Basin was conducted using pointwise data of maximum horizontal stress (S_{Hmax}). The data were plotted against depth, and the mean orientation of S_{Hmax} , along with the standard deviation, was calculated for each 100-depth interval. No. of boreholes represent the number of boreholes with S_{Hmax} indicators in each interval. The results show that the S_{Hmax} orientation remains consistent across different depth intervals, with only small variations observed (approximately 15° to 25°, which is within the standard deviation) above and below 700 m. These slight variations at shallower intervals can be attributed to data density (see the no. of datapoints and boreholes) and the inherent uncertainty in stress data analysis.

5. Discussion

5.1. Stress orientation in northern Bowen Basin

This study resulted in a comprehensive stress orientation map for northern Bowen Basin (Fig. 5). Notably, Fig. 6 demonstrates a high degree of consistency in the mean S_{Hmax} orientation across various qualities and types of data throughout the study area. For example, based on 153 A-C quality data records, the mean S_{Hmax} orientation for the study area was determined to be $N018^\circ \pm 16^\circ$. Remarkably, this value is similar to the mean S_{Hmax} orientation calculated using 659 A-D quality data, which resulted in $N020^\circ \pm 19^\circ$. These outcomes highlight the robustness and reliability of the stress orientation data across different datasets, reaffirming the consistent stress pattern observed throughout the northern Bowen Basin.

The majority of borehole data used in this study were obtained from open-pit mines (see Table 1), which are shallow with small coverage of borehole image logs. This resulted in a substantial number of D-quality data, which is considered as less reliable S_{Hmax} data records according to the World Stress Map ranking scheme.⁴⁰ Previous studies in eastern Australian basins such as southern Bowen, Sydney, Surat, and Gunnedah have indicated that D-quality data records often represent a deviating local stress pattern.^{5,79} However, contrasting findings have been observed in other basins within Australia,⁵ as well as in the Moatize Basin in Mozambique,⁵⁷ Taranaki Basin in New Zealand,¹⁷ Geothermal wells in Iceland,⁸⁰ Western Canadian basins,⁸¹ and Southeast Asia.⁸² In these cases, D-quality data may not necessarily serve as indicators of localized stress and could instead represent regional stress patterns. Hence, extreme caution is required to work with D-quality data for basin stress analysis.¹⁷ Note that D-quality data can arise due to a high standard deviation of mean S_{Hmax} (i.e., between $\pm 25^\circ$ and $\pm 40^\circ$) within a borehole or due to limited occurrences of BO/DIF (i.e., <4 distinct breakouts or <20 m combined length in a single borehole).

In our statistical analysis, we examined various sets of data with different qualities and found that the mean S_{Hmax} orientation of the study area did not show significant differences (Fig. 6). Even when considering only 506 D-quality data records, the calculated mean S_{Hmax} orientation for the study area was $N022^\circ \pm 20^\circ$, which closely resembles the mean S_{Hmax} from A-C quality data (i.e., $N018^\circ \pm 16^\circ$) and is well within the inherent uncertainties. This similarity is further supported by the wavelength analysis of stress data for both A-C and A-D quality data, showing comparable results (Fig. 7a and c). Upon reviewing our database, it becomes evident that the majority of boreholes received a D-quality due to the limited occurrence of BO/DIF (i.e., <4 distinct breakouts or <20 m combined length in a single borehole), rather than a high standard deviation. Only 21 boreholes with D-quality exhibited a standard deviation of $>25^\circ$ (Fig. 9). Consequently, our findings reveal a consistent mean S_{Hmax} orientation in the northern Bowen Basin, regardless of the inclusion of D-quality data.

5.2. Observational stress data and large-scale geomechanical models' predictions

The pattern of S_{Hmax} orientation in most Australian basins is well-documented in the published literature. However, there is a noticeable scarcity of stress information for some regions, such as northern Bowen Basin, despite it being recognized as a rich basin for energy and resources.^{20,22} Prior to this study, some researchers have worked on the stress state of northern Bowen Basin, however, the limited S_{Hmax} orientation, in the public domain, means that the stress pattern in this part of the Bowen Basin is poorly understood. Understanding the stress pattern in northern Bowen Basin is particularly significant given that detailed stress analyses in different Australian sedimentary basins have revealed various scenarios for stress pattern. For example, some basins, such as Darling, Cooper-Eromanga, Bonaparte, Gippsland, and Otway, display homogeneous S_{Hmax} orientations, while others, including

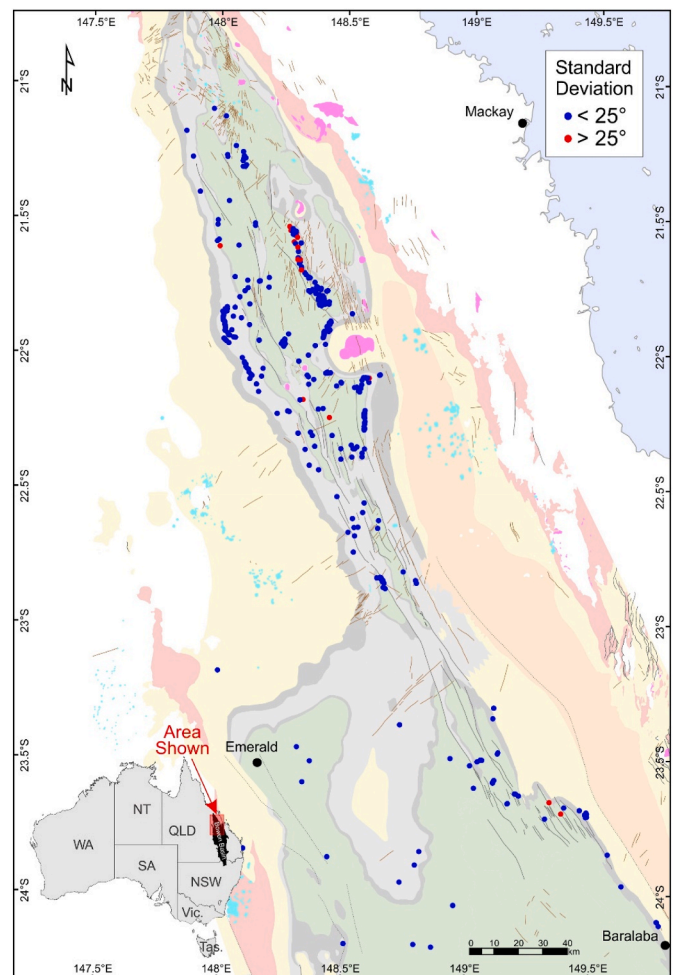


Fig. 9. Distribution of D-quality data and their corresponding standard deviations in our study area. The majority of the D-quality data exhibits a standard deviation of less than 25° . See Fig. 2 for the map legend.

Sydney, Gunnedah, Surat, Browse, and some parts of the Carnarvon basins, exhibit variable stress patterns.^{5,9,11,15} Hence, characterizing the stress pattern of the northern Bowen Basin becomes crucial to determine if it is affected by localized perturbations, similar to what has been observed in the southern Bowen and Surat basins.^{5,9-11} By shedding light on the stress pattern of this region, this study aims to contribute valuable insights to the overall understanding of the tectonics and geomechanical characteristics of the northern Bowen Basin.

Early studies on the stress pattern of northern Bowen Basin were conducted as part of larger investigations aimed at analysing the stress patterns of the entire Bowen Basin and eastern Australian basins. For instance, the analysis of hydraulic fracturing testing and overcoring measurements revealed that the mean S_{Hmax} orientation for the entire Bowen Basin is $N16^\circ E \pm 27^\circ$.^{8,12,14,15,50,83,84} These studies revealed that the mean S_{Hmax} orientation in northern Bowen Basin is $N007^\circ E \pm 23^\circ$. Reynolds⁵⁰ further investigated the stress analysis of the Bowen Basin using detailed statistical analysis. It was suggested that although the S_{Hmax} orientation remains consistent over most of the Bowen Basin, there is a slight easterly rotation in the S_{Hmax} orientation between the northern and southern regions of the basin.

Tavener et al.,¹¹ examined 145 borehole data to explore the stress pattern of the Bowen and Surat basins. The findings of their investigation suggested significant variability in the S_{Hmax} orientation across their study area, leading to the identification of six sub-regions for the S_{Hmax} azimuth. According to Tavener et al.,¹¹ northern Bowen Basin shows $N022^\circ E \pm 19^\circ$ orientation for the S_{Hmax} that gradually rotates to $N070^\circ E$

$\pm 34^\circ$ in south-central Bowen and then $N090^\circ E \pm 04^\circ$ in southern Bowen Basin. It should be noted that Tavener et al.,¹¹ defined their region for the northern Bowen Basin as approximately between latitudes of -24.00 and -25.00 . In contrast, in our current study, we define the northern Bowen Basin as spanning from latitude -21.00 down to -24.36 . Consequently, only two S_{Hmax} data records from Tavener et al.,¹¹ fall within the boundaries of our database for the northern Bowen Basin.

Before this study, there was limited stress information available for the northern Bowen Basin, particularly in the far northern region, where it is an active mining area but has seen relatively limited exploration for deeper coal seam gas compared to the southern part of the basin (Fig. 1). In the absence of observational data, our understanding of the *in-situ* stress pattern in the region has mainly relied on geomechanical models of stress for the Australian tectonic plate. Several studies, as detailed by Rajabi et al.,⁷ have attempted to investigate the regional stress pattern of Australia by constructing 2D and 3D geomechanical-numerical models at continental and tectonic plate scales. These published models have presented various patterns for the S_{Hmax} orientation in the northern Bowen Basin. For example, Reynolds et al.,¹⁸ utilized a 2D plate-scale model and predicted a regional pattern of NNE-SSW and NE-SW for northern Bowen Basin. Burbidge⁸⁵ suggested a NE-SW orientation of the S_{Hmax} azimuth (in a normal faulting stress regime). On the other hand, 2D plate-scale models by Dyksterhuis et al.,⁸⁶ and Müller et al.,⁸⁷ proposed a NW-SE trend for the S_{Hmax} azimuth in the northern Bowen Basin. Given these divergent model predictions, this study contributes new observational data to evaluate the previously published models and gain insights into the factors influencing the stress pattern of northeastern Australia. By providing fresh observational data, this research allows for a more comprehensive assessment of the role of different forces on the stress pattern of the region.

5.3. Controls on the stress pattern of northern Bowen Basin

Over the past three decades, extensive analysis and modelling of the *in-situ* stress pattern in the Australian continent have revealed that the regional stress pattern (i.e., on scales greater than 500 km) is primarily controlled by tectonic plate boundary forces.^{7,18,86–88} However, when it comes to basin scales, detailed *in-situ* stress analysis has shown that the stress patterns of some basins cannot be solely described by plate tectonic forces, and additional forces at smaller scales (i.e., on scales less than 500 km) are required to explain the observed stress variability.^{5,9,11,15,89} Therefore, it is crucial to understand whether the stress pattern of the northern Bowen Basin is similar to basins that exhibit consistent S_{Hmax} orientation at the basin scale or if it displays significant stress variability.

As discussed earlier, this study has revealed a mean S_{Hmax} orientation of $N020^\circ \pm 19^\circ$, which demonstrates a considerable level of consistency across the northern Bowen Basin (Figs. 5–7). Rajabi et al.,⁷ conducted a comprehensive evaluation of various plate-scale geomechanical models of stress for Australia and found that the model developed by Reynolds et al.,¹⁸ exhibited the least deviation when compared to the observational mean S_{Hmax} orientation in the Australian stress provinces. Remarkably, the stress analysis conducted in this study also demonstrates a remarkable agreement between the S_{Hmax} orientation inferred from borehole data and the predictions provided by the 2D geomechanical-numerical model proposed by Reynolds et al.¹⁸

Our study area is situated in the northern part of the Australian plate, in close proximity to the Tonga Kermadec, Solomon Trench, New Hebrides, and Papua New Guinea regions (Fig. 1). The geographic proximity of the northern Bowen Basin to the boundaries of the Australian and Pacific tectonic plates underscores the potential impact of these plate boundaries on the stress pattern of northeastern Australia, including the Bowen Basin.⁵⁰ The 2D plate-scale geomechanical model developed by Reynolds et al.,¹⁸ suggests that compression resulting from the

interactions at the New Hebrides and Solomon boundaries leads to a prevailing NNE-SSW orientation for S_{Hmax} in the Bowen Basin region.^{18,50} Therefore, as proposed by Reynolds,⁵⁰ the interplay between the Australian and Pacific plates at the boundaries of Hebrides and Solomon plays a crucial role in shaping the regional pattern of present-day stress in the northern Bowen Basin.

As outlined above, the stress orientation in the northern Bowen Basin exhibits no systematic rotation, and the regional stress pattern is primarily governed by plate tectonic forces. However, there are some variabilities in some regions both spatially and with depth. For example, Fig. 10 shows some perturbed S_{Hmax} orientation in the northern part of our study area, where the geology is more complex and variations in basement topography are observed.²¹ It is worth noting that geological and basement structures have been identified as key factors contributing to stress variabilities in eastern Australian sedimentary basins.^{6,9–11,13,79,90} In addition to spatial variations in stress patterns, we have also observed numerous depth-wise, small-scale rotation of stress (i.e., <500 m) in some of the boreholes, particularly in close proximity to faults, abrupt changes in lithology, and massive fracture zones (Fig. 11). These depth-wise stress variations suggest the influence of local geological features and structural complexities on stress distribution in the northern Bowen Basin. These findings underscore the significance of incorporating geological information and subsurface

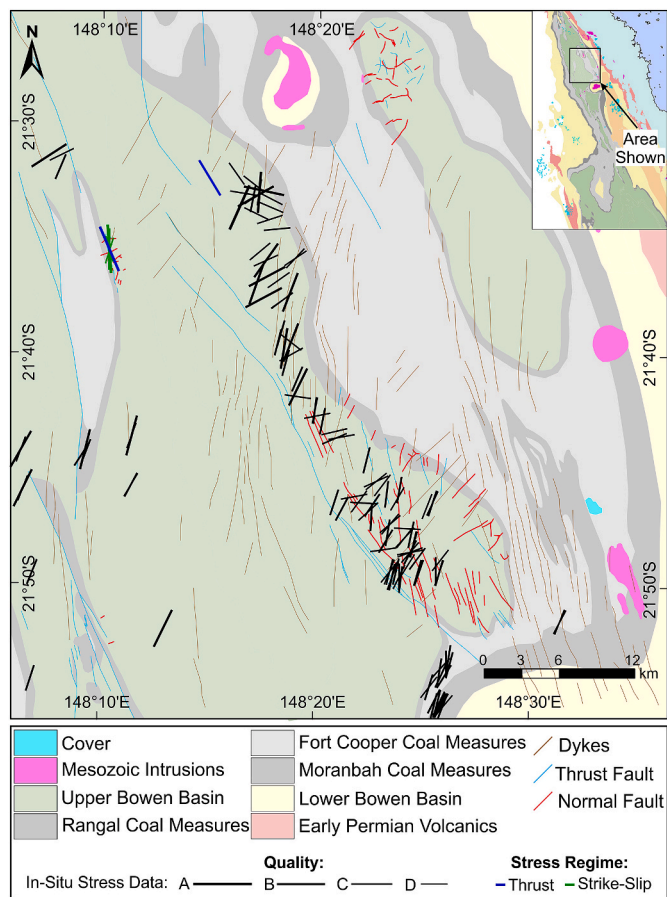


Fig. 10. Variable pattern of maximum horizontal stress (S_{Hmax}) orientation, depicted by black lines, in northern part of the study area. As shown by Rajabi et al.,²¹ this part of the basin represents the changes in basement topography and also contains extensive swarms of dykes (purple lines). These stiff/hard materials could be a possible cause of stress variability in this region. Note that most of the stress azimuth data in this region are assigned as D-quality due to low number of breakouts in each borehole (see Fig. 9). (For interpretation of the references to colour in this figure legend, the reader is referred to the Web version of this article.)

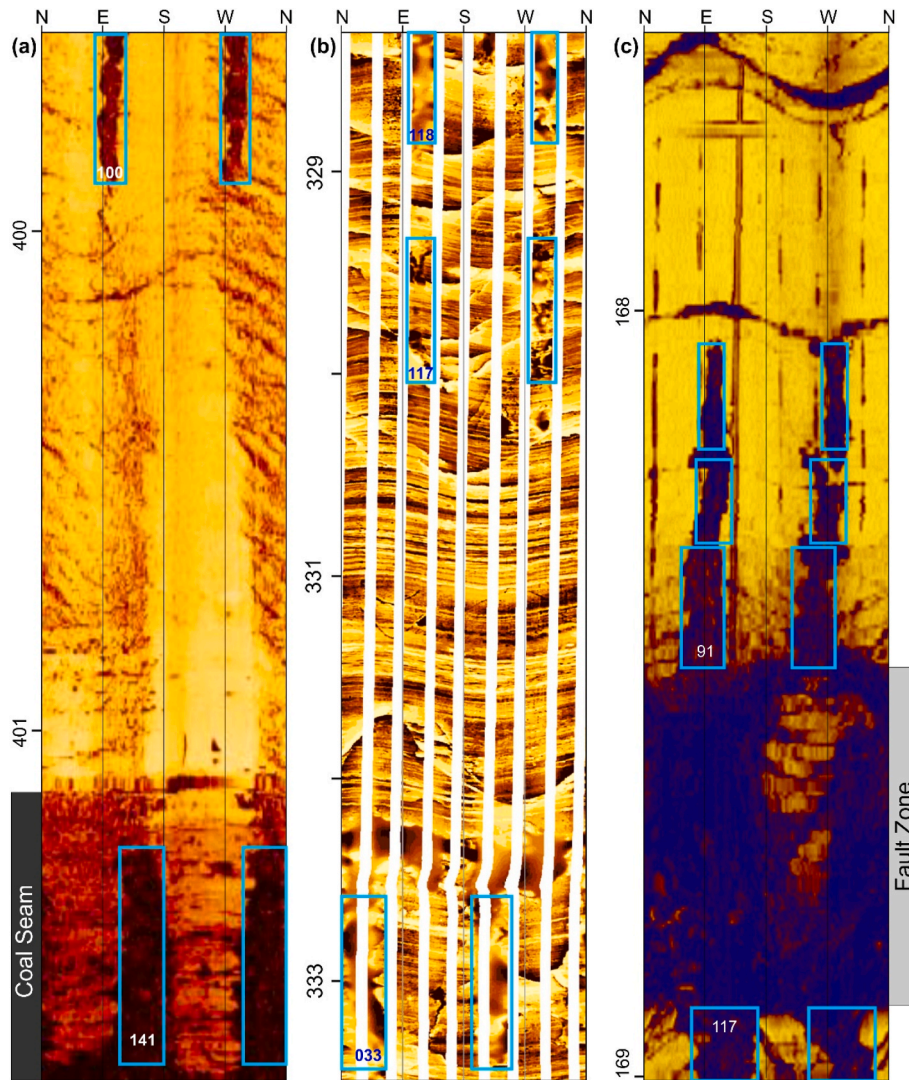


Fig. 11. Examples of borehole breakouts (BOs) rotations in some of the studied boreholes. Note that BOs outlined in blue and numbers next to them represent their orientations. (a) Acoustic televiewer log shows 40° of breakout rotation from 141° in coal seam (darker intervals) to 100° in interburden (lighter interval). As there are no major faults between these two intervals, it can be concluded that elastic contrast probably perturbs stress orientation in this example. (b) Shows 85° rotation of breakouts (from 033° to 118°) in a resistivity-based image log. Between these intervals there are several faults that can possibly explain the rotation. (c) Shows an acoustic televiewer log that shows ~26° rotation of BOs below and above a minor fault zone. (For interpretation of the references to colour in this figure legend, the reader is referred to the Web version of this article.)

structures in understanding the stress pattern of the region, particularly in areas where geological complexities play a prominent role in influencing stress distribution.

One of the central inquiries addressed in this paper was whether the *in-situ* stress variability in the northern Bowen Basin resembles that of the southern Bowen and Surat basins. Through our detailed stress mapping efforts, which have resulted in the development of one of the most detailed and quality-ranked basin-scale stress maps worldwide, we have found a consistent S_{Hmax} orientation across the entirety of the northern Bowen Basin. Furthermore, our study revealed the presence of stress variabilities at smaller scales, particularly in regions characterized by complex geology and significant changes in basement topography (Figs. 10 and 11). The remarkable consistency of S_{Hmax} orientation in the northern Bowen Basin, when compared to the southern Bowen and Surat basins, is also evident in our search-radii statistical analysis. As depicted in Fig. 7, there is a gradual decrease in the wavelength of S_{Hmax} azimuth from north to south. This observation implies that S_{Hmax} orientation exhibits a notably large wavelength in the northern parts of the basin, signifying a consistent stress orientation over substantial distance. As we

move towards the southern part, the wavelength decreases, indicating that S_{Hmax} orientation remains consistent over shorter distances in this region and more local perturbations occur.

6. Conclusions

Prior to undertaking this study, the Australian Stress Map database had a limited reliable open-file *in-situ* stress data records for the northern Bowen Basin. However, our comprehensive analysis of borehole data has led to a significant expansion of S_{Hmax} data records, reaching a total of 890 records. These data were derived from an in-depth examination of 128 km of borehole image logs retrieved from 680 vertical boreholes.

The statistical analysis of the S_{Hmax} data demonstrated that the mean S_{Hmax} orientation in the northern Bowen Basin is N020°E, with a standard deviation of $\pm 19^\circ$. This mean S_{Hmax} orientation displays strong spatial and depth consistency. Moreover, the agreement between the observed mean S_{Hmax} orientation in this study and the predicted S_{Hmax} orientation using a plate-scale geomechanical model emphasizes the significant influence of plate boundary forces on the stress pattern in the

northern Bowen Basin. This pattern stands in contrast to most of the eastern Australian basins, such as the Surat, southern Bowen, Gunnedah, and Sydney basins, which display considerable stress variabilities at different scales due to the interaction of various forces.

While the regional S_{Hmax} orientation in the northern Bowen Basin generally aligns with the NNE direction, small-scale stress rotations (ranging from 1 to 10 km) have been identified in regions with changes in basement topography and complex geology. Furthermore, detailed borehole image log analysis in this study uncovered very small-scale stress rotations (occurring between 1 and 10 m) in some boreholes. These rotations were attributed to stiffness contrasts caused by changes in lithology and the presence of geological structures.

CRedit authorship contribution statement

Mojtaba Rajabi: Conceptualization, Data curation, Formal analysis, Funding acquisition, Investigation, Methodology, Project administration, Resources, Software, Supervision, Validation, Visualization, Writing – original draft, Writing – review & editing. **Moritz Ziegler:** Conceptualization, Formal analysis, Writing – review & editing. **Oliver Heidbach:** Conceptualization, Supervision, Writing – review & editing. **Saswata Mukherjee:** Conceptualization, Formal analysis, Writing – review & editing, Investigation. **Joan Esterle:** Conceptualization, Data curation, Funding acquisition, Writing – review & editing.

Declaration of competing interest

The authors declare that they have no known competing financial interests or personal relationships that could have appeared to influence the work reported in this paper.

Data availability

All the results are available as online supplementary materials. However, the raw well log data are confidential.

Acknowledgments

The authors gratefully thank two anonymous reviewers for their time and constructive comments. This work has been supported by ACARP (project no. C29011). The authors would like to thank Anglo American, Fitzroy Australia Resources, and Peabody Energy Australia for their data contribution and permission to publish the results of this study. We also would like to thank the Geological Survey of Queensland for the open file CSG data used in the study. The authors extend their gratitude to Ikon Science, Aspentech-Subsurface Science & Engineering (Paradigm Geophysical Corp.), and Advanced Logic Technology for their generous support, i.e., providing academic licenses for the software packages used in this study.

Appendix A. Supplementary data

Supplementary data to this article can be found online at <https://doi.org/10.1016/j.ijrmms.2023.105630>.

References

- Talwani P. *Intraplate Earthquake*. New York: Cambridge University Press; 2014:332.
- Talwani P. On the nature of intraplate earthquakes. *J Seismol*. 2016;1–22.
- Assumpção M, Dias FL, Zevallos I, Naliboff JB. Intraplate stress field in South America from earthquake focal mechanisms. *J S Am Earth Sci*. 2016;71:278–295.
- Cloetingh S. Intraplate stresses: a new element in basin analysis. In: Kleinspehn KL, Paola C, eds. *New Perspectives in Basin Analysis*. New York, NY: Springer New York; 1988:205–230.
- Rajabi M, Tingay M, Heidbach O, Hillis R, Reynolds S. The present-day stress field of Australia. *Earth Sci Rev*. 2017;168:165–189.
- Heidbach O, Rajabi M, Cui C, et al. The World Stress Map database release 2016: crustal stress pattern across scales. *Tectonophysics*. 2018;744:484–498.
- Rajabi M, Heidbach O, Tingay M, Reiter K. Prediction of the present-day stress field in the Australian continental crust using 3D geomechanical-numerical models. *Aust J Earth Sci*. 2017;64(4):435–454.
- Hillis R, Reynolds SD. In: *In Situ Stress Field of Australia*. vol. 372. Geological Society of America Special Papers; 2003:49–58.
- Mukherjee S, Rajabi M, Esterle J, Copley J. Subsurface fractures, in-situ stress and permeability variations in the Walloon coal measures, eastern Surat Basin, Queensland, Australia. *Int J Coal Geol*. 2020;222C, 103449.
- Brooke-Barnett S, Flottmann T, Paul PK, et al. Influence of basement structures on in situ stresses over the Surat Basin, southeast Queensland. *J Geophys Res Solid Earth*. 2015;120(7):4946–4965.
- Tavener E, Flottmann T, Brooke-Barnett S. In: *In Situ Stress Distribution and Mechanical Stratigraphy in the Bowen and Surat Basins*. vol. 458. Queensland, Australia: Geological Society, London, Special Publications; 2017. SP458.454.
- Evere JR, Mallett CW. *Stress Measurements in the Bowen Basin and Their Relationship to the Structural Setting of the Basin*. Kingscote, Kangaroo Island: Geological Society of Australia Inc; 1989:40–41.
- Rajabi M, Tingay M, King R, Heidbach O. Present-day stress orientation in the Clarence-Moreton Basin of New South Wales, Australia: a new high density dataset reveals local stress rotations. *Basin Res*. 2017;29(S1):622–640.
- Evere JR, Hillis R, Reynolds S. *The Regional Stress Field in Eastern Australian Sedimentary Basins and its Relevance to Mining and Civil Engineering*. *Earth Stress and Industry: The World Stress Map and beyond*. Heidelberg, Germany: Heidelberg Academy of Sciences and Humanities, Geophysical Institute, University of Karlsruhe; 1998, 15–15.
- Hillis R, Evere JR, Reynolds SD. In situ stress field of eastern Australia. *Aust J Earth Sci*. 1999;46(5):813–825.
- Salmachi A, Rajabi M, Reynolds P, Yarmohammadtooski Z, Wainman C. The effect of magmatic intrusions on coalbed methane reservoir characteristics: a case study from the Hoskissons coalbed, Gunnedah Basin, Australia. *Int J Coal Geol*. 2016;165: 278–289.
- Rajabi M, Ziegler M, Tingay M, Heidbach O, Reynolds S. Contemporary tectonic stress pattern of the Taranaki Basin, New Zealand. *J Geophys Res Solid Earth*. 2016; 121(8):6053–6070.
- Reynolds SD, Coblenz DD, Hillis R. Tectonic forces controlling the regional intraplate stress field in continental Australia: results from new finite element modeling. *J Geophys Res Solid Earth*. 2002;107(B7). ETG 1-1-ETG 1-15.
- Tozer B, Sandwell DT, Smith WHF, Olson C, Beale JR, Wessel P. Global bathymetry and topography at 15 arc sec: SRTM15+. *Earth Space Sci*. 2019;6(10):1847–1864.
- Colclough H, Pheeney J. *Australian Operating Mines Map 2022*. 23rd Edition. Canberra: Geoscience Australia; 2022. Scale 1:7,000,000.
- Rajabi M, Sliwa R, Esterle J. Integrating in-situ stress patterns with basin to local scale structures in the Nebo Synclinorium, Bowen Basin. *ACARP Report C29011*. 2023:120.
- Salmachi A, Rajabi M, Wainman C, et al. History, geology, in situ stress pattern, gas content and permeability of coal seam gas basins in Australia: a review. *Energies*. 2021;14(9):2651.
- Rajabi M. The present-day state of tectonic stress in eastern Australia. In: *3rd AEGC: Geosciences for a Sustainable World*. Australian Society of Exploration Geophysicists; 2021:1–4. <https://doi.org/10.5281/zenodo.7690572>. Online.
- Lee MF, de Vries R, Moller CF. Rock stresses, its controls and associated ground behaviour at the Rosebery mine, Tasmania. In: Wesseloo J, ed. *Deep Mining 2017: Eighth International Conference on Deep and High Stress Mining*. Perth: Australian Centre for Geomechanics; 2017:901–916.
- Simmons JV. Geomechanics of Australian open cut coal mining. In: Dight PM, ed. *International Symposium on Slope Stability in Open Pit Mining and Civil Engineering*. Perth: Australian Centre for Geomechanics; 2020:39–64.
- Jaeger JC, Cook NGW, Zimmerman R. *Fundamentals of Rock Mechanics*. fourth ed. Oxford: Wiley-Blackwell; 2007.
- Brady BHG, Brown ET. *Rock Mechanics*. 3 ed. Springer Netherlands; 2006.
- Ulusay R. *The ISRM Suggested Methods for Rock Characterization*. Testing and Monitoring; 2015, 2007–2014.
- Ziegler M, Reiter K, Heidbach O, et al. Mining-induced stress transfer and its relation to a Mw 1.9 seismic event in an ultra-deep South African gold mine. *Pure Appl Geophys*. 2015;172(10):2557–2570.
- Rajabi M, Tingay M, Heidbach O. The present-day state of tectonic stress in the Darling Basin, Australia: implications for exploration and production. *Mar Petrol Geol*. 2016;77:776–790.
- Barton CA, Zoback MD, Moos D. Fluid flow along potentially active faults in crystalline rock. *Geology*. 1995;23(8):683–686.
- Ziegler M, Heidbach O. Manual of the matlab script Stress2Grid v1.1. *WSM Technical Report 19-02-GFZ Data Services*; 2019: 33. <http://doi.org/10.2312/wsm2019002>.
- Babaahmadi A, Sliwa R, Esterle J, Rosenbaum G. The development of a Triassic fold-thrust belt in a synclinal depositional system, Bowen Basin (eastern Australia). *Tectonics*. 2017;36(1):51–77.
- Sliwa R, Babaahmadi A, Esterle J. *Structure Supermodel 2017 - Fault Characterisation in Permian to Jurassic Coal Measures, Eastern Australia*. . ACARP End of Grant Report C24032. 2018:50.
- Brakel AT, Totterdell JM, Wells AT, Nicoll MG. Sequence stratigraphy and fill history of the Bowen Basin, Queensland. *Aust J Earth Sci*. 2009;56(3):401–432.
- Salmachi A, Zeinijahromi A, Algarni MS, et al. Experimental study of the impact of CO2 injection on the pore structure of coal: a case study from the Bowen Basin, Australia. *Int J Coal Geol*. 2023;275, 104314.
- Wang X, Holmes C, Khalili AD, Esterle J. Assessment of CO2 storage capability in denison trough, Bowen Basin. *The APPEA Journal*. 2023;63:336–348.

38. Boreham CJ, Golding SD, Glikson M. Factors controlling the origin of gas in Australian Bowen Basin coals. *Org Geochem*. 1998;29(1):347–362.
39. Bradshaw BE, Spencer LK, Lahtinen A-L, et al. An assessment of Queensland's CO2 geological storage prospectivity — the Queensland CO2 Geological Storage Atlas. *Energy Proc*. 2011;4:4583–4590.
40. Heidbach O, Tingay M, Barth A, Reinecker J, Kurfeß D, Müller B. Global crustal stress pattern based on the World Stress Map database release 2008. *Tectonophysics*. 2010;482(1–4):3–15.
41. Veevers JJ. *Billion-year Earth History of Australia and Neighbours in Gondwanaland*. Sydney, N.S.W., Australia: Gemoc Press; 2000.
42. Donchak PTJ, Purdy DJ, Withnall IW, Blake PR, Jell PA. New england orogen (chapter 5). In: Jell PA, ed. *Geology of Queensland*. Brisbane, Australia: Geological Survey of Queensland; 2013:305–472.
43. Murray CG. Tectonic evolution and metallogenesis of the Bowen Basin. In: *Bowen Basin Symposium 1990*. Mackay, Queensland, Australia: Proceedings of the Geological Society of Australia (Queensland Division); 1990:201–212.
44. Korsch RJ, Totterdell JM, Cathro DL, Nicoll MG. Early permian east Australian rift system. *Aust J Earth Sci*. 2009;56(3):381–400.
45. Fielding CR, Falkner AJ, Scott SG. Fluvial response to foreland basin overfilling; the late permian rangal coal measures in the Bowen Basin, Queensland, Australia. *Sediment Geol*. 1993;85(1):475–497.
46. Holcombe RJ, Stephens CJ, Fielding CR, et al. *Tectonic Evolution of the Northern New England Fold Belt: The Permian-Triassic Hunter-Bowen Event*. Geological Society of Australia, Special Publications; 1997.
47. Korsch RJ, Totterdell JM, Fomin T, Nicoll MG. Contractional structures and deformational events in the bowen, Gunnedah and Surat basins, eastern Australia. *Aust J Earth Sci*. 2009;56(3):477–499.
48. Cook AG, Bryan SE, Draper J. Post-orogenic Mesozoic basins and magmatism. In: Jell PA, ed. *Geology of Queensland: Queensland*. Brisbane, Australia: Geological Survey of Queensland; 2013:515–575.
49. Cook AG, Jell JS. Paleogene and neogene (chapter 8). In: Jell PA, ed. *Geology of Queensland*. Brisbane, Australia: Geological Survey of Queensland; 2013:577–652.
50. Reynolds SD. *Characterization and Modelling of the Regional In Situ Stress Field of Continental Australia*. National Centre for Petroleum Geology and Geophysics. Adelaide: The University of Adelaide; 2001:216. PhD.
51. Engelder T. *Stress Regimes in the Lithosphere*. New Jersey: Princeton University Press; 1993.
52. Schmitt DR, Currie CA, Zhang L. Crustal stress determination from boreholes and rock cores: fundamental principles. *Tectonophysics*. 2012;580(0):1–26.
53. Zoback MD. *Reservoir Geomechanics*. New York: Cambridge University Press; 2007.
54. Morawietz S, Heidbach O, Reiter K, et al. An open-access stress magnitude database for Germany and adjacent regions. *Geoth Energy*. 2020;8(1):25.
55. Bohnsack D, Drews M, Duschl F, Shatyrbayeva I, Heidbach O, Müller B. *A Subsurface Pore Pressure Map of Bavaria from Quality-Ranked Borehole Data - a Template for Europe and beyond*. Berlin: European Geothermal Congress 2022; 2022:1–6.
56. Ranjbar-Karami R, Rajabi M, Ghavidel A, Afroogh A. Contemporary tectonic stress pattern of the Persian Gulf Basin, Iran. *Tectonophysics*. 2019;766:219–231.
57. Rajabi M, Esterle J, Heidbach O, Travassos D, Fumo S. Characterizing the contemporary stress orientations near an active continental rift zone: a case study from the Moatize Basin, central Mozambique. *Basin Res*. 2022;34(4):1292–1313.
58. Sbar ML, Sykes LR. Contemporary compressive stress and seismicity in eastern North America: an example of intra-plate tectonics. *Geol Soc Am Bull*. 1973;84(6):1861–1882.
59. Voight B, Taylor JW, Voight JP. Tectonophysical implications of rock stress determinations. *Geol Rundsch*. 1968;58(2):655–676.
60. Zoback ML. First- and second-order patterns of stress in the lithosphere: the world stress map project. *J Geophys Res Solid Earth*. 1992;97(B8):11703–11728.
61. Mardia KV. *Statistics of Directional Data*. London ; New York: Academic Press; 1972.
62. Rajabi M, Sherkatli S, Bohloli B, Tingay M. Subsurface fracture analysis and determination of in-situ stress direction using FMI logs: an example from the Santonian carbonates (Ilam Formation) in the Abadan Plain, Iran. *Tectonophysics*. 2010;492(1–4):192–200.
63. Mukherjee S, Rajabi M, Esterle J. Relationship between coal composition, fracture abundance and initial reservoir permeability: a case study in the Walloon Coal Measures, Surat Basin, Australia. *Int J Coal Geol*. 2021;240, 103726.
64. Laubach SE, Baumgardner Jr RW, Monson ER, Hunt E, Meador KJ. Fracture detection in low-permeability reservoir sandstone: a comparison of BHTV and FMS logs to core. In: *SPE Annual Technical Conference and Exhibition*. Houston: Texas Society of Petroleum Engineers; 1988:11.
65. Prensley SE. Advances in borehole imaging technology and applications. *Geological Society, London, Special Publications*. 1999;159(1):1–43.
66. Bell JS, Gough DI. Northeast-southwest compressive stress in Alberta evidence from oil wells. *Earth Planet Sci Lett*. 1979;45(2):475–482.
67. Mastin L. Effect of borehole deviation on breakout orientations. *J Geophys Res Solid Earth*. 1988;93(B8):9187–9195.
68. Pell S, Straub K. Orientation data from acoustic scanner logs: a case study comparing manual interpretation with automated software. In: *Bowen Basin Symposium-2021*. Mackay, QLD: Bowen Basin Geologist's Group; 2021.
69. Roshan H, Li D, Canbulat I, Regenauer-Lieb K. Borehole deformation based in situ stress estimation using televiwer data. *J Rock Mech Geotech Eng*. 2023;15(9):2475–2481.
70. Coblenz D, Richardson RM. Statistical trends in the intraplate stress field. *J Geophys Res Solid Earth*. 1995;100(B10):20245–20255.
71. Müller B, Wehrle V, Hettel S, Sperner B, Fuchs K. A new method for smoothing orientated data and its application to stress data. *Geological Society, London, Special Publications*. 2003;209(1):107–126.
72. Hansen KM, Mount VS. Smoothing and extrapolation of crustal stress orientation measurements. *J Geophys Res Solid Earth*. 1990;95(B2):1155–1165.
73. Ziegler MO, Heidbach O. The 3D stress state from geomechanical-numerical modelling and its uncertainties: a case study in the Bavarian Molasse Basin. *Geoth Energy*. 2020;8(1):11.
74. Heidbach O, Barth A, Müller B, et al. WSM quality ranking scheme, database description and analysis guidelines for stress indicator. *World Stress Map Technical Report 16-01, GFZ German Research Centre for Geosciences*; 2016. <http://doi.org/10.2312/wsm2016001>.
75. Pierdominici S, Heidbach O. Stress field of Italy — mean stress orientation at different depths and wave-length of the stress pattern. *Tectonophysics*. 2012;532–535(0):301–311.
76. Tingay M, Bentham P, De Feyter A, Kellner A. Present-day stress-field rotations associated with evaporites in the offshore Nile Delta. *Geol Soc Am Bull*. 2011;123(5-6):1171–1180.
77. Fejerskov M, Lindholm C, Myrvang A, Bungum H. Crustal stress in and around Norway: a compilation of in situ stress observations. *Geological Society, London, Special Publications*. 2000;167(1):441–449.
78. Bell JS. Petro Geoscience 2. In situ stresses in sedimentary rocks (part 2): applications of stress measurements. *Geosci Can*. 1996;23(3):135–153.
79. Rajabi M, Tingay M, Heidbach O. The present-day stress field of New South Wales, Australia. *Aust J Earth Sci*. 2016;63(1):1–21.
80. Ziegler M, Rajabi M, Heidbach O, et al. The stress pattern of Iceland. *Tectonophysics*. 2016;674:101–113.
81. Reiter K, Heidbach O, Schmitt D, Haug K, Ziegler M, Moeck I. A revised crustal stress orientation database for Canada. *Tectonophysics*. 2014;636:111–124.
82. Tingay M, Morley C, King R, Hillis R, Coblenz DD, Hall R. Present-day stress field of southeast asia. *Tectonophysics*. 2010;482(1–4):92–104.
83. Enever J, Wooltorton B, Edgoose J, Bride J, Sullivan D. *Notes Accompanying Summary of Bowen Basin Stress Measurements, Map and Notes*. Melbourne: CSIRO Division of Geomechanics; 1989.
84. Enever JR, Pattison CI, McWatters RH, Clark IH. The relationship between in-situ stress and reservoir permeability as a component in developing an exploration strategy for coalbed methane in Australia. EUROCK '94. In: *SPE-ISM Rock Mechanics in Petroleum Engineering*. Balkema, Rotterdam: Society of Petroleum Engineers; 1994:163–171.
85. Burbidge DR. Thin plate neotectonic models of the Australian plate. *J Geophys Res Solid Earth*. 2004;109(B10), B10405.
86. Dyksterhuis S, Albert RA, Müller RD. Finite-element modelling of contemporary and palaeo-intraplate stress using ABAQUS™. *Comput Geosci*. 2005;31(3):297–307.
87. Müller RD, Dyksterhuis S, Rey P. Australian paleo-stress fields and tectonic reactivation over the past 100 Ma. *Aust J Earth Sci*. 2012;59(1):13–28.
88. Coblenz D, Zhou S, Hillis R, Richardson RM, Sandiford M. Topography, boundary forces, and the Indo-Australian intraplate stress field. *J Geophys Res Solid Earth*. 1998;103(B1):919–931.
89. Bailey AHE, Jarrett AJM, Tenthorey E, Henson PA. Understanding present-day stress in the onshore canning basin of western Australia. *Aust J Earth Sci*. 2021;68(6):818–838.
90. Gale WJ, Enever JR, Blackwood RL, McKay J. *An Investigation of the Effect of a Fault/ monocline Structure on the In-Situ Stress Field and Mining Conditions at Nattai Bulli Colliery NSW, Australia*. CSIRO Australia, Division of Geomechanics, Geomechanics of Coal Mining Report No 48; 1984.